ELSEVIER

Thermochimica Acta 398 (2003) 233–240

thermochimica acta

www.elsevier.com/locate/tca

Thermal behaviors of mechanically activated pyrites by thermogravimetry (TG)

Huiping Hu*, Qiyuan Chen, Zhoulan Yin, Pingmin Zhang

Institute of Chemistry and Chemical Engineering, Central South University, Changsha 410083, PR China

Received 11 March 2002; received in revised form 8 July 2002; accepted 9 July 2002

Abstract

The thermal decompositions of mechanically activated and non-activated pyrites were studied by thermogravimetry (TG) at the heating rate of 10 K min^{-1} in argon. Results indicate that the initial temperature of thermal decomposition (T_{di}) in TG curves for mechanically activated pyrites decreases gradually with increasing the grinding time. The specific granulometric surface area (S_G), the structural disorder of mechanically activated pyrites were analyzed by X-ray diffraction laser particle size analyzer, and X-ray powder diffraction analysis (XRD), respectively. The results show that the S_G of mechanically activated pyrites remains almost constant after a certain grinding time, and lattice distortions (ε) rise but the crystallite sizes (D) decrease with increasing the grinding time. All these results imply that the decrease of T_{di} in TG curves of mechanically activated pyrites is mainly caused by the increase of lattice distortions ε and the decrease of the crystallite sizes D of mechanically activated pyrite with increasing the grinding time. The differences in the reactivity between non-activated and mechanically activated pyrites were observed using characterization of the products obtained from 1 h treatment of non-activated and mechanically activated pyrites at 713 K under inert atmosphere and characterization of non-activated and mechanically activated pyrites exposed to ambient air for a certain period.

Keywords: TG measurement; Mechanical activation; Pyrite; Thermal decomposition; Exposure to ambient air

1. Introduction

Pyrite (FeS_2) is a very common sulphide mineral and is found in a wide range of geological sites [1], and is one of the most common gold-bearing sulphide minerals [1,2]. But pyrite is one of the refractory minerals [3]. It has been known for some time that the reactivity of minerals can be improved by grinding—a process known as 'mechanical activation'. For example, ultrafine grinding of chalcopyrite increases its activity so that less severe leaching conditions are required to recover the copper [4,5]. Thus the term 'mechanical activation' refers to mechanically induced enhancement of the chemical reactivity of a system [6]. The best way to study mechanochemical transformation of the mechanical activation for ores is to analyze in situ the milled mixture using appropriate spectroscopic methods, since chemical handling can obscure the true nature of the initial products. But nowadays, most common tools are IR and X-ray powder diffraction (XRD) techniques, which normally allow the identification of the products [7,8]. Other techniques like HREM, EXFAM, X-ray photoelectron spectra (XPS), and X-ray cyclotron resonance, etc.,

* Corresponding author.
E-mail addresses: pqfang@cs.hn.cn, hhuiping@mail.csu.edu.cn (H. Hu).

0040-6031/03/$ – see front matter © 2002 Published by Elsevier Science B.V.
PII: S0040-6031(02)00390-8

have been used to study the new surfaces of the milled products [9]. For example, Baláž et al. [10] investigated the changes produced in cinnabar by its mechanical activation in a planetary mill through XPS, BET, XRD, and DSC. And the DSC curves of mechanically activated cinnabars and non-activated cinnabar represent an association of endothermic effects, which differ from each other in shape and values of the extreme temperatures. But except for our previous work [11], few concerns have been made on the thermal stability of mechanically activated sulphide ores using thermogravimetry (TG).

In this paper, mechanically activated pyrites were studied using the TG–DTGA technique under a dynamic argon atmosphere. The structural changes of non-activated and mechanically activated pyrites after 1 h of treatment at 713 K under inert atmosphere, or after exposure to ambient air were examined. And the differences in reactivity between non-activated and mechanically activated pyrites are also discussed.

2. Experimental

Natural pyrite ore was purchased from a domestic geological museum, and its chemical compositions are presented in Table 1. It was found by X-ray diffraction analysis that the natural pyrite contained cubic pyrite as a predominant component. The non-activated pyrite was prepared by crushing the natural pyrite in a jaw crusher to a particle size of $\leq$1 mm, then stored in air for more than 1 year. The non-activated pyrite (10 g) was added into a stainless vessel with six stainless steel balls of 18 mm in diameter and 12 balls of 8 mm in diameter, then kept in higher vacuum (the residue pressure $\leq$1 Pa), followed by bubbling highly pure nitrogen into this vessel through an inlet of this vessel for half-an-hour, and this operation was performed once again (i.e., non-activated pyrite was kept under an inert atmosphere), and then mechanically activated in a planetary ball mill (QM-ISP Planetary Mill, PR China) under a rotation rate of 200 rpm. A powder-to-ball mass ratio of 1:25 was employed, and mechanically activated pyrites were obtained after grinding for grinding time t_G = 20, 40, 120 and 260 min. Non-activated pyrite and the pyrite mechanically activated under inert atmosphere for 20 min were exposed to air at ambient temperature for a certain period.

The measurements pertaining to TG were performed by using a thermal analyzer TGA/SDTA 851^e (Mettler Toledo, USA and Switzerland) with temperature program from 25 to 1000 °C at the heating rate of 10 K min^{-1} under highly pure argon with flowing rate of 70 ml min^{-1}. The sample mass is almost 34 mg.

Non-activated and mechanically activated pyrites (the latter was milled for 40 min in inert atmosphere) were treated for 1 h in an oven at 713 K under flowing pure nitrogen (70 ml min^{-1}), the products were obtained and characterized by X-ray diffraction phase analysis, respectively.

XRD profiles from the milled powders were recorded on a 3014 diffractometer (Rigaku, Japan) using Cu Kα radiation (λ = 1.54 Å, voltage 40 kV, current 20 mA) with time constant 0.5 s, limit of measurement, 10 impulses s^{-1}, and step size of 0.03°. The recorded XRD spectra were used for calculation of the degree of structural disorder—the distortion (ε) of crystal lattice (presented as a percentage) and the crystallite size (D) was also observed, which was determined from the changes in profile of the diffraction peaks [12], such as (2 2 0) and (5 5 1) planes of different pyrites. As the increase of the profile breadths mainly results from the increase of the lattice distortion ε and the decrease of the crystallite size D, ε and D can be calculated by using the model of Gaussian function [13].

Table 1
The chemical analyses of the natural pyrite

	Elements									
	Fe	S	Si	Ca	Sn	Sb	As	Zn	Co	Ni
Content (wt.%)	45.63	52.38	0.1	0.01	0.01	0.01	0.03	0.05	0.005	0.001

The specific granulometric surface area (S_G), of mechanically activated pyrites was calculated statistically from the corresponding particle size distribution data measured on a Mastersizer 2000 Laser Diffraction Particle Size Analyzer (Malvern, UK), and distilled water was used as a dispersing agent.

XPS were obtained with a KRATOS XSAM800 X-ray photoelectron spectrometer, with a monochromatized Mg Kα X-ray source. The operating pressure in the analyzer chamber was $\leq 2 \times 10^{-7}$ Pa. The energy scale was calibrated using the Fermi edge and the $4f_{7/2}$ line (BE = 84.0 eV) for gold. The surface charge was measured relative to uncharged graphite C 1s at 284.6 eV.

3. Results and discussion

3.1. TG and DTGA curves for non-activated and mechanically activated pyrites

The TG and DTGA curves for non-activated and mechanically activated pyrites were obtained (Fig. 1A and B). And the initial temperatures of thermal decomposition in the TG curves were presented in Table 2.

Table 2 shows that T_{di} in the TG curves for non-activated and mechanically activated pyrites decreases gradually with increasing the grinding time. Therefore, the reactivity of mechanically activated pyrite is higher than that of non-activated pyrite.

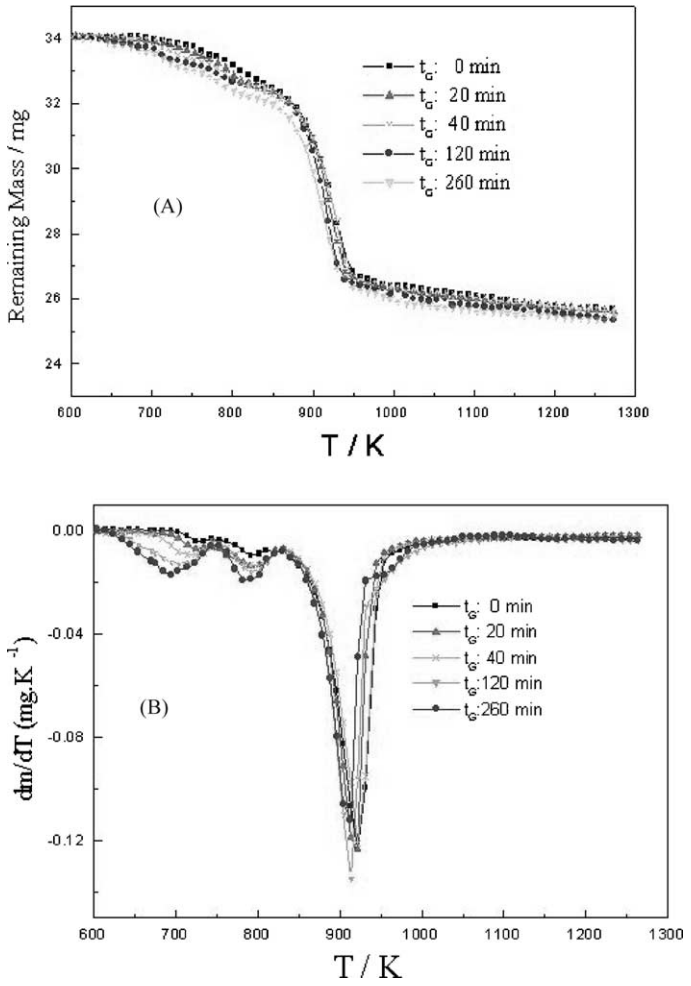

Fig. 1. TG–DTGA curves for non-activated and mechanically activated pyrites: (A) TG curves for non-activated and mechanically activated pyrites; (B) DTGA curves for non-activated and mechanically activated pyrites.

Table 2
The relationship between the initial temperature of thermal decomposition (T_{di}) for non-activated and mechanically activated pyrites and grinding time (t_G)

	t_G (min)				
	0	20	40	120	260
T_{di} (K)	713	705.5	690	648	635

3.2. Additional surpports for the opinion that the reactivity of mechanically activated pyrite is higher than that of non-activated pyrite

The products were obtained from the 1 h treatment of non-activated and mechanically activated pyrites (the latter was milled for 40 min in inert atmosphere) in an oven at 713 K under flowing pure nitrogen, respectively, followed by being characterized by X-ray diffraction phase analysis (shown in Fig. 2). Fig. 2 shows the products obtained from the 1 h treatment of mechanically activated pyrite contain more monoclinic pyrrhotite formed than that of non-activated pyrite. This is an additional support for the above opinion.

There is another observation that non-activated pyrite and the pyrite mechanically activated under inert atmosphere for 20 min without exposure or after exposure to ambient air for 3 and 6 months, or 1 year were characterized by XRD, and XPS, respectively, which is also an support for the above opinion. The XRD spectra of non-activated pyrites without exposure or after exposure to ambient air for 3 or 6 months or 1 year are almost overlapped, but XRD spectra for mechanically activated pyrites after exposure to

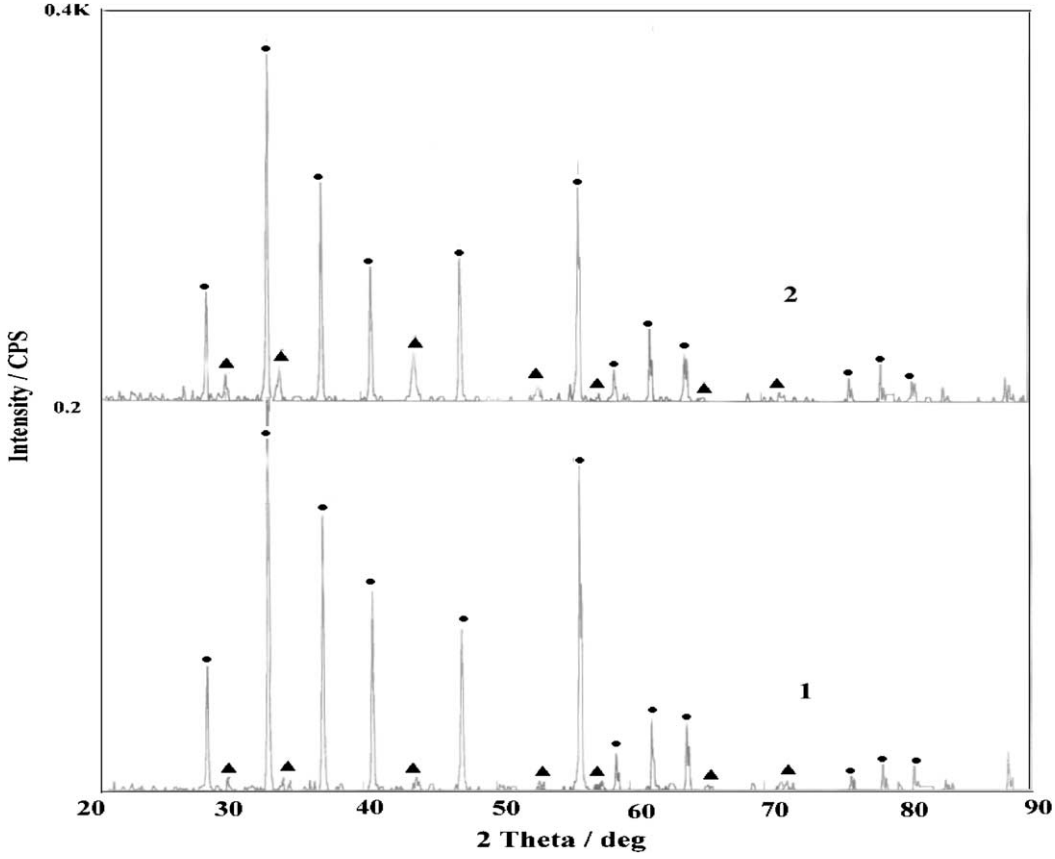

Fig. 2. XRD patterns for the products treated from non-activated and activated pyrites: (1) products obtained from non-activated pyrite; (2) products obtained from mechanically activated pyrite. (●) Volume-centered cubic pyrite; (▲) monoclinic pyrrhotite.

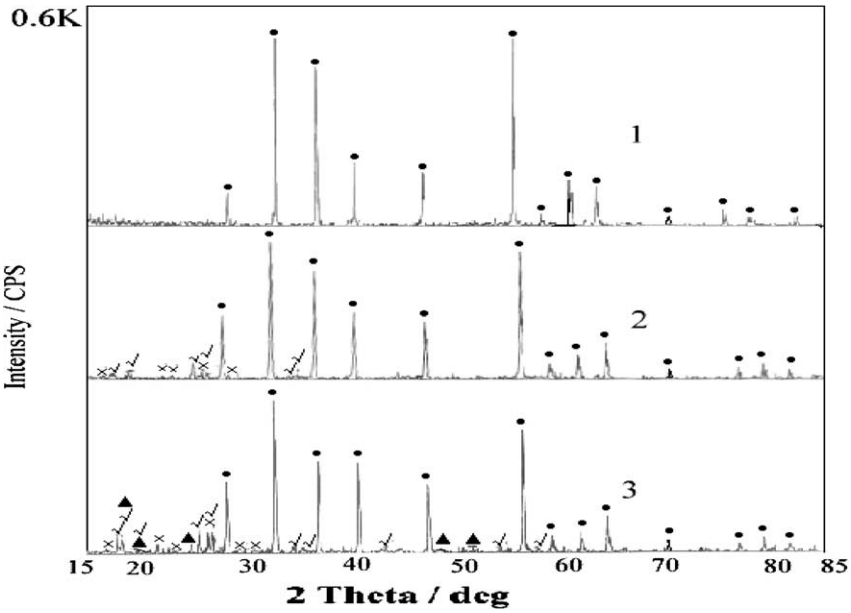

Fig. 3. XRD spectra of different exposed pyrites: (1) non-activated pyrite without exposure or after exposure to ambient air for 1 year and the pyrite mechanically activated under inert atmosphere for 20 min; (2) the pyrite mechanically activated under inert atmosphere for 20 min, followed by being exposed to ambient air for 3 months; (3) the pyrite mechanically activated under inert atmosphere for 20 min, followed by being exposed to ambient air for 6 months. (●) Pyrite; (√-) $FeSO_4·H_2O$; (×) $Fe_3(SO_4)_4·14H_2O$; (▲) $Fe_2(SO_4)_3·H_2O$.

ambient air are different (shown in Fig. 3). Fig. 3 shows that when non-activated and mechanically activated pyrites were exposed to ambient air for 3 and 6 months, or 1 year, only mechanically activated pyrites were oxidized with air to produce oxidation products, such as $FeSO_4·H_2O$, $Fe_3(SO_4)_4·14H_2O$ and $Fe_2(SO_4)_3·H_2O$.

XPS spectra of non-activated pyrite and the pyrite mechanically activated under inert atmosphere for 20 min after exposure to ambient air are listed in Figs. 4 and 5. XPS spectra of non-activated pyrites without exposure or after exposure to ambient air for 1 year and mechanically activated pyrite without exposure are the same. Because the mechanical activation of the samples in this experiment was performed under inert atmosphere, we can overlook oxidation reaction of sulphide ores with air during mechanical activation. Figs. 4 and 5 illustrate, respectively, the significant differences in both shape and binding energy of the Fe 2p and S 2p XPS spectrum of mechanically activated pyrite exposed to ambient air for 6 months compared to those of non-activated pyrite exposed to

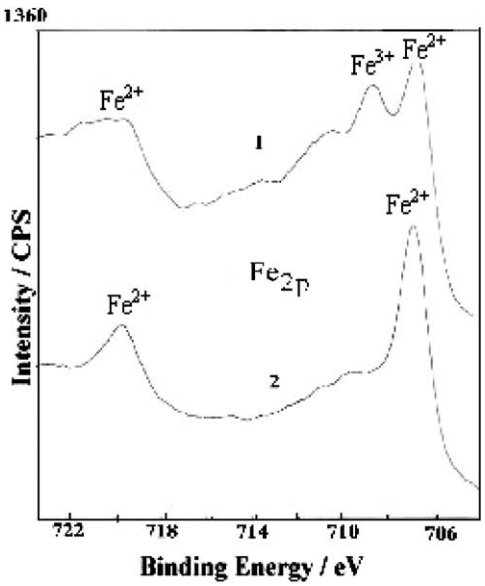

Fig. 4. XPS Fe 2p spectra of exposed pyrites (1) mechanically activated pyrite exposed to ambient air for 6 months, and (2) non-activated pyrite exposed to ambient air for 1 year.

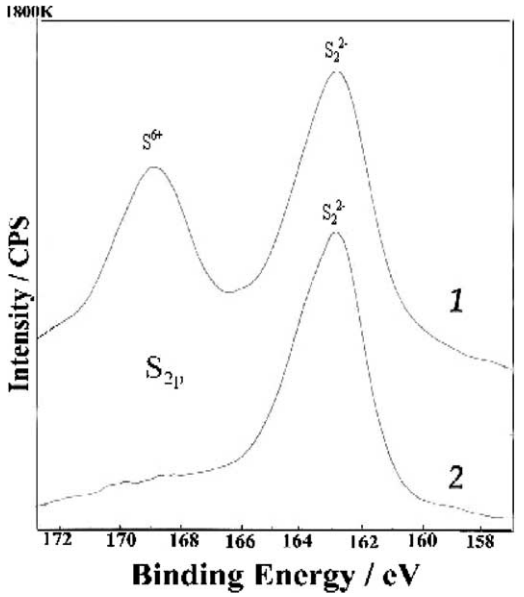

Fig. 5. XPS S 2p spectra of exposed pyrites (1) mechanically activated pyrite exposed to ambient air for 6 months, and (2) non-activated pyrite exposed to ambient air for 1 year.

ambient air for 1 year. One new XPS Fe 2p and S 2p peak occurred in the range 708–709, and 168–170 eV, respectively. The corresponding S 2p binding energies 163.2 and 169.3 eV were for pyrite S_2^{2-} species [14] and S^{6+} species of SO_4^{2-} [15] and the corresponding energies 706.6 and 708.6 eV were for Fe^{2+} species of pyrite or $FeSO_4{\cdot}H_2O$ [16] and Fe^{3+} species of $Fe_3(SO_4)_4{\cdot}14H_2O$ or $Fe_2(SO_4)_3{\cdot}H_2O$.

The differences in the reactivity between non-activated and mechanically activated pyrites result from the differences in the surface structure between them. It is well-known that mechanical activation, which results in the formation of metastable solids [17], is a means of accelerating the leaching process for sulfidic ores. Contributing to the success of these technique are [18–20]: (1) increased surface area; (2) the microstructural modifications stemming from the deformation; (3) chemical reaction.

The S_G of mechanically activated pyrites are shown in Fig. 6. Fig. 6 shows that the S_G of mechanically activated pyrites remain almost constant after $t_G > 200$ min, which implies that the increase of the structural disorder and chemical reaction may mainly result in the decrease of T_{di} in the TG curves for mechanically activated pyrites.

3.3. Study on the changes of structural order of non-activated and mechanically activated pyrites

By analyzing X-ray diffraction peaks (2 2 0) and (5 5 1) of non-activated and mechanically activated pyrites, the values of D and ε are obtained (see Table 3) and X-ray diffraction peaks (2 2 0) and (5 5 1) for different pyrites are also listed in Figs. 7 and 8, accordingly.

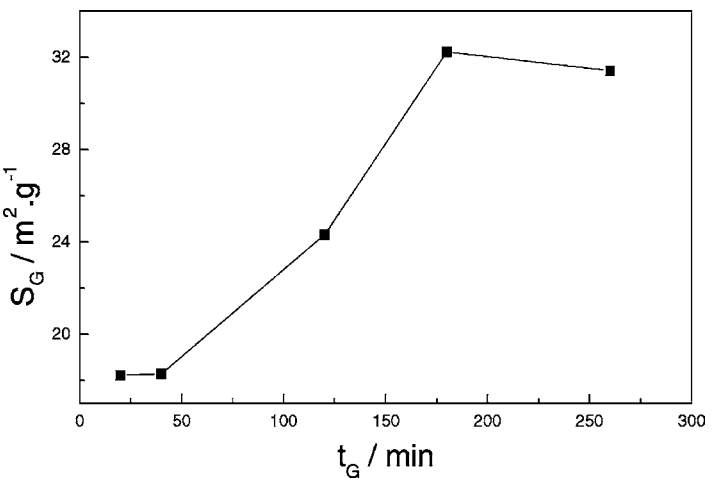

Fig. 6. The specific granulometric surface area (S_G), of mechanically activated pyrites versus the grinding time.

Table 3
The relationship between D, and ε of mechanically activated pyrites and grinding time t_G

	t_G (min)				
	0	20	40	120	260
D (Å)	4032	2988	675	564	544
ε (%)	0	0.03	0.05	0.06	0.07

Table 3 shows that the crystallite sizes D decrease and the deformations of the crystal ε increase gradually with increasing the grinding time, which is similar with the study of mechanically activated chalcopyrite, galena and pyrite [11,21].

3.4. Study on the chemical reaction during mechanical activation of sulphide ores

The mechanical activation of the samples in this experiment was performed under inert atmosphere, we can overlook oxidation reaction of sulphide ores with air during mechanical activation.

Therefore, non-activated pyrite undergoes the structural distortion of pyrites during mechanical activation in inert atmosphere during grinding, which leads to the formation of metastable pyrite. The metastable pyrites containing accumulated excess energy can thermally decompose more easily than non-activated pyrite, and this structural sensitivity of thermal decomposition of mechanically activated pyrites confirms that of chalcopyrite, and galena [11,17].

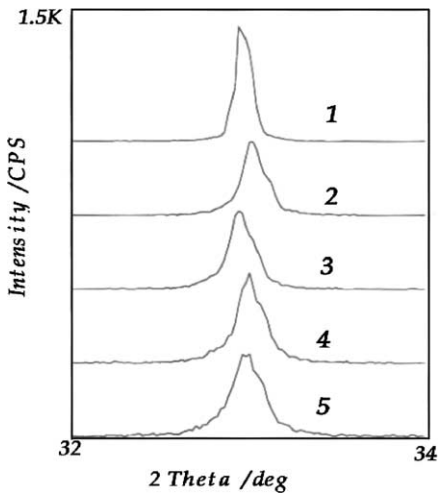

Fig. 7. Peaks (2 2 0) of X-ray diffraction patterns for different pyrites after different grinding time: (1) $t_G = 0$ min; (2) $t_G = 20$ min; (3) $t_G = 40$ min; (4) $t_G = 120$ min; (5) $t_G = 260$ min.

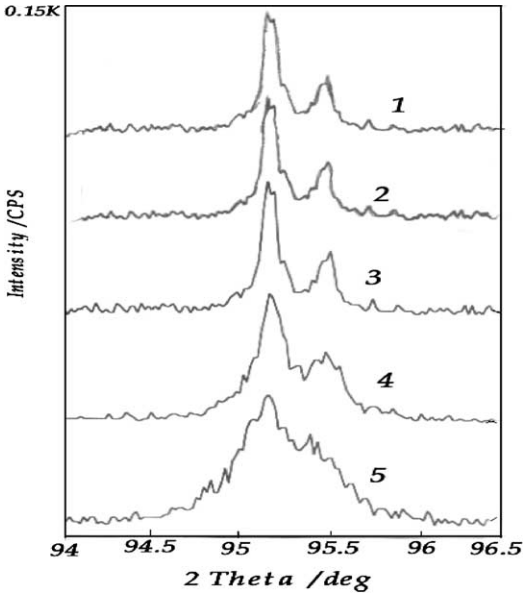

Fig. 8. Peaks (5 5 1) of X-ray diffraction patterns for different pyrites after different grinding time: (1) $t_G = 0$ min; (2) $t_G = 20$ min; (3) $t_G = 40$ min; (4) $t_G = 120$ min; (5) $t_G = 260$ min.

4. Conclusions

The initial temperature of thermal decomposition for pyrites in the TG curves decreases gradually with increasing the grinding time of mechanically activated pyrites, which results from the increases of the structural disorder during the mechanical activation of pyrites under inert atmosphere. Mechanically activated pyrite is more easily subjected to thermal decomposition than non-activated pyrite. It can be concluded that TG is a useful indirect method for the characterization of mechanically activated pyrites.

Acknowledgements

The authors gratefully acknowledged the financial support from the Key Project 59934080 of the National Natural Science Foundation of China and the National

Doctorate Program Fund 20000053321 of the State Education Committee of China.

References

[1] J.B. Hiskey, P.P. Phule, M.D. Pritzker, Metall. Mater. Trans. B 18 (1987) 641.
[2] J.B. Hiskey, M.D. Pritzker, J. Appl. Electrochem. 18 (1988) 484.
[3] M.N. Lehmann, S. O'Leary, J.G. Dunn, Miner. Eng. 13 (1) (2000) 1–18.
[4] E. Gock, Erzmetall. 31 (1978) 282–288.
[5] I.J. Corrans, J.E. Angove, Miner. Eng. 4 (7–11) (1991) 763–776.
[6] C.J. Warris, P.G. McCormick, Miner. Eng. 10 (10) (1997) 1119–1125.
[7] K. Sasaki, H. Konno, M. Inagaki, J. Mater. Sci. 29 (1994) 1666–1669.
[8] I. Persson, P. Persson, M. Valli, S. Fózó, B. Malmensten, Int. J. Process. 33 (1991) 67–81.
[9] J.F. Fernández-Bertran, Pure Appl. Chem. 71 (4) (1999) 581–586.
[10] P. Baláž, E. Post, Z. Bastl, Thermochim. Acta 200 (1992) 371–377.
[11] H. Hu, Q. Chen, Z. Yin, P. Zhang, Thermochim. Acta (2002), in press.
[12] R.A. Varin, J. Bystrzycki, A. Calka, Intermetallics 7 (1999) 785–796.
[13] H.P. Klug, L. Alexander, X-ray Diffraction Procedures for Polycrystalline and Amorphous Materials, second ed., Wiley, New York, 1974, Chapter 9, pp. 618–708.
[14] J.R. Mycroft, G.M. Bancroft, N.S. Mclntyre, J.W. Lorimer, I.R. Hill, J. Electroanal. Chem. 292 (1990) 139–152.
[15] M.K. Yelloji Rao, K.A. Natarajan, Int. J. Miner. Process. 29 (1990) 175–194.
[16] D. Brion, Appl. Surf. Sci. 5 (1980) 133–152.
[17] V.V. Boldyrev, Proc. Indian Nat. Sci. Acad., Part A 52 (1986) 400.
[18] K. Laajalehto, I. Kartio, E. Suoninen, Int. J. Miner. Process. 51 (1997) 163–170.
[19] D. Maurice, J.A. Hawk, Hydrometallurgy 49 (1998) 103–123.
[20] J.F. Fernández-Bertran, Pure Appl. Chem. 71 (4) (1999) 581–586.
[21] L. Honggui, Y. Jiahong, Z. Zhongwei, J. Central South Univ. Technol. 29 (1) (1998) 28–31 (in Chinese).